Malaya Journal of Matematik, Vol. 6, No. 2, 435-442, 2018

https://doi.org/10.26637/MJM0602/0022

# Numerical study of fluid flow and heat transfer in a backward facing step with a rotating cylinder

A. Anguraj [1]* and J. Palraj [2]

**Abstract**

The present study analyzes the laminar flow and heat transfer over a backward-facing step with an adiabatic rotating cylinder in a channel. The governing Navier-Stokes and energy equations are solved using finite element method. The effect of Reynolds number, cylinder rotation angle and various cross-stream positions of the cylinder on the fluid flow and heat transfer characteristics of the backward-facing step flow have been studied numerically. The working fluid is assigned a Prandtl number of 0.71 throughout this investigation. The flow and thermal fields have been explained by streamline and isotherm profiles respectively. It is observed that the flow field and heat transfer rate are influenced by the variations of these parameters. Furthermore, the length and size of the wake zones can be controlled with cylinder rotation angles.

**Keywords**

Navier-Stokes equations; Rotating obstacle; Backward facing step; finite element method; Recirculation length; Heat transfer.

**AMS Subject Classification**

78M10, 65L60, 76U99, 76D10, 76D05.

[1] *Department of Mathematics, PSG College of Arts and Science, Tamil Nadu, India.*

[2] *Department of Mathematics, PSG College of Technology, Tamil Nadu, India.*

***Corresponding author**: [1] angurajpsg@yahoo.co.in; [2] palrajpsg@gmail.com

**Article History**: Received **24** October **2017**; Accepted **09** February **2018**



## Contents



## 1. Introduction

The flow separation, recirculation and following reattachment which occurs in many engineering applications. A backward or forward facing step, has an important role in optimizing a wide variety of many engineering applications where as heating or cooling is required, due to the sudden changes in flow geometry in critical components. Such complex flow structures are present in many applications such as inside combustors, collectors of power systems, flow in valves, cooling of nuclear reactors, wide angle diffusers and nuclear reactor due to generate separation and reattachment region, as well as in external flows such as flow around aircraft, airfoils, buildings, cooling systems for electronic equipment, heat exchangers, chemical process, power plants, energy system equipment, cooling passages for turbine blades, industrial ducts, gas turbine engines, chemical processes and many other devices of heat transfer.

This flow separation and reattachment of the flow almost always determines the key structure of the flow field and significantly influences the mechanism of heat transfer in these devices because of the the great dealing of mixing of high and low fluid energy.

**Nomenclature**

| | |
|---|---|
| c | temperature, K |
| $C_p$ | specific heat, J/kg K |
| D | diameter of the cylinder, m |
| H | width of the channel, m |
| h | local heat transfer coefficient, $Wm^{-2}K^{-1}$ |
| k | thermal conductivity, $Wm^{-1}K^{-1}$ |
| ER | channel expansion ratio, H/(H-S) |
| $L_1$ | downstream length of the channel, m |
| $L_2$ | step size, m |
| $L_3$ | upstream length of the step, m |
| n | unit normal vector |
| Nu | local Nusselt number, hH/k |
| $\bar{Nu}$ | spatial-averaged Nusselt number |
| p | pressure, Pa |
| $Pr$ | Prandtl number, $\mu C_p/k$ |
| $S$ | Step size, m |
| Re | Reynolds number, $UH/\nu$ |
| t | time, s |
| u | x-component velocity, $ms^{-1}$ |
| v | y-component velocity, $ms^{-1}$ |
| x,y | cartesian coordinates, m |
| a,b | cylinder position, m |

Greek Symbols

| | |
|---|---|
| $\rho$ | density, $kgm^{-3}$ |
| $\nu$ | kinematic viscosity, $m^2s^{-1}$ |
| $\omega$ | cylinder rotation angle. |

Flow through backward or forward facing step channel leads to generate separation, recirculation and reattachment. The backward or forward facing step geometry is very simple, yet the flow and the heat transfer through it contain most of the features encountered in more complex geometries, it is easy to set-up both experimentally and computationally. Owing to its simple geometry, Some studies focused on the heat transfer phenomena over the backward and forward-facing step flow geometry has received a great deal of attention in the literature in the past decades both experimentally [1, 2, 4, 5] and numerically [6–8] to obtain the basic information of the flow separation and reattachment phenomena flow regime.

Armaly et al. [3] investigated the relationship between the Reynolds number and reattachment length by both experimentally and as well as numerically studied for laminar, transition and turbulent air flow over backward-facing step (for the range of Reynolds number $70 < Re < 8000$). They found that the separation length increase with increase of the Reynolds number for $Re < 1200$ while reduction at Re between 1200 to 5500. Sherry et al. [4] have made an experimental investigation for the recirculation zone formed downstream of a forward facing step immersed in a turbulent boundary layer. In their study, the mechanisms effecting the reattachment distance is discussed.

Numerical Studies have also been conducted for the flow over a backward facing or forward facing step. Nie and Armaly [7] present a numerical study of three-dimensional laminar forced flow adjacent to backward-facing step placed in rectangular duct. The results demonstrated that the maximum reattachment length occurs at the sidewall and not at the center of the duct and as the step height increases the maximum Nusselt number increases. Barbosa-Saldana and Anand [8] have numerically studied the 3D laminar flow over a horizontal forward-facing step. The expansion ratio and aspect ratio of two and four is considered. Effects of the Reynolds number on the locations of the reattachment line, velocity distribution and averaged Nusselt number are discussed.

In addition, used obstacle in flow passage leads to increase the static pressure and then enhance the heat transfer. In 1988 Williamson stated that the flow past a circular cylinder undergoes several interesting changes with Reynolds number. The temperature limitation on the electronic equipments in order to maintain their reliability and accuracy has led to consider the problem of thermal management of electronic devices. Due to its importance, a vast amount of literature is dedicated to the study of forced convection flow in a channel with heated blocks.

Several studies have been conducted to investigate the laminar forced and mixed convection flow in enclosures with rotating or stationary cylinders both experimentally and numerically [9]. In [9] Rehimi et al. have studied experimentally the flow past a circular cylinder located between parallel walls for the range of Reynolds number between 30 and 277. They reported differences between the unconfined cylinder case and their results shows that von-Karman instability is shifted to a large value Reynolds number for the confined cylinder case. In [10] Hussain and Hussein have numerically did the mixed convection in an enclosure with a rotating cylinder using a finite volume method. They observed and showed that the rotating cylinder locations have an important effect in enhancing convection heat transfer in the square enclosure.

Heat transfer and fluid flow characteristics over a backward facing or forward facing step in a channel with the insertion of obstacles has received some attention in the literature [11–14]. Oztop et al. [12] have numerically studied the turbulent forced convection of double forward facing step with obstacles. They put rectangular obstacles before each step and investigated the effects of step height, obstacle aspect ratio and Reynolds number on fluid flow and heat transfer. They reported that heat transfer rate increases when the obstacle aspect ratio increases. Kumar and Dhiman [13] have numerically studied the heat transfer enhancement in laminar forced convection flow over a backward facing step with the insertion of an adiabatic circular cylinder. They considered different cross-stream positions of the circular cylinder for the Reynolds number between 1 and 200. They obtained heat transfer enhancement up to 155 compared to no-cylinder case. Lin et al. [14] analyzed numerically mixed convective heat transfer results for laminar, buoyancyassisting, two-dimensional flow in a vertical duct with a backward-facing step for a wide range of inlet flow and wall temperature con-

ditions. The authors presented in their work the velocity and temperature distributions along with Nusselt numbers and wall skin friction coefficient for wide ranges of flow and temperature parameters.

Theoretical, analytical and experimental studies of backward or forward facing step flow have been presented by many researchers. To the authors knowledge, a backward-facing step with an adiabatic rotating cylinder in a channel is not investigated yet and the lack of such results motivated the current study. The objective of the present study is to numerical simulation of fluid flow and heat transfer over a backward facing step with and without the presence of an adiabatic rotating cylinder is performed for the range of Reynolds number ($1 \leq Re \leq 200$), cylinder rotation angle ($-3 \leq \omega \leq 3$) and obstacle location ($b = 0.5S, S, 1.5S$).

## 2. Mathematical formulation of the problem

In this section, the computational domain and configurations of the obstacle are presented. A schematic description of the physical problem is shown in Fig 1. A channel with a backward facing step is considered, the step size $L_2$ of the backward facing step is S and channel height $L_4$ is 2S. The downstream distance $L_1$ between the edge of the step and the exit plane of the domain is taken as 40S and the upstream distance $L_3$ between the inlet plane and the step edge is taken as 10S. It is well known that the flow separation and recirculation cause very poor heat transfer characteristics in the region near the step. To alter the hydrodynamic and thermal characteristics, an adiabatic rotating circular cylinder is placed behind the step for three different vertical locations within the channel. The center of the circular cylinder with diameter D=0.4 is located at $(a,b)$ where a = 0.6 and b = 0.5S, S, 1.5S. A uniform velocity (U=1) and a uniform temperature ($T_I = 0$) are assumed to enter the inflow boundary $\Gamma_1$ and pressure is set to zero at the outflow boundary $\Gamma_3$. The downstream bottom surface $\Gamma_4$ of the backward facing step is maintained at constant temperature $T_c$ which is higher then the inlet temperature $T_I$, while the other wall boundarys ($\Gamma_2, \Gamma_5, \Gamma_6$ and $\Gamma_7$) of the channel are treated as no slip boundarys with adiabatic condition. Working fluid is air with a Prandtl number Pr=0.71. The flow is assumed to be two dimensional, Newtonion, incompressible and in the laminar flow regime.

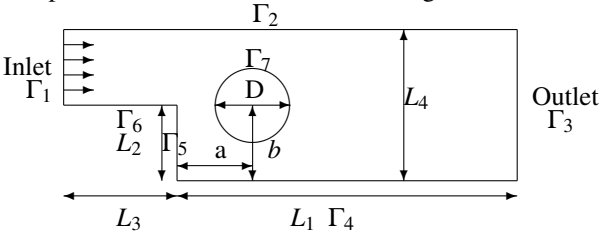


**Figure 1**

The governing equations for two dimensional, incompressible, laminar and unsteady case can be written as follows,

Continuity equation

$$\operatorname{div} \mathbf{u} = 0 \tag{2.1}$$

Momentum equation

$$\frac{\partial \mathbf{u}}{\partial t} + \mathbf{u} \cdot \nabla \mathbf{u} = -\nabla p + \frac{1}{Re} \Delta \mathbf{u} \tag{2.2}$$

Energy equation

$$\frac{\partial c}{\partial t} + \mathbf{u} \cdot \nabla c = \frac{1}{RePr} \Delta c \tag{2.3}$$

where c is temperature.

The boundary conditions can be given as follows,

At the inflow boundary($\Gamma_1$), velocity is unidirectional and temperature is uniform

$$u = U \quad v = 0 \quad c = 0 \tag{2.4}$$

At the bottom wall($\Gamma_4$), downstream of the backward-facing step, temperature is constant (C=1)

On the channel walls(except $\Gamma_4$), adiabatic wall with no-slip boundary conditions are assumed

$$u = 0, \quad v = 0, \quad \frac{\partial c}{\partial n} = 0 \tag{2.5}$$

where $n$ denote the surface normal directions

On the cylinder surface($\Gamma_7$), an adiabatic wall boundary condition is used and specified velocity components is $u = -\omega(y - y_0)$, $v = \omega(x - x_0)$, $\frac{\partial c}{\partial n} = 0$.

At the out flow boundary($\Gamma_3$),

$$\frac{\partial u}{\partial x} = 0, \quad \frac{\partial v}{\partial x} = 0, \quad \frac{\partial c}{\partial x} = 0 \tag{2.6}$$

The governing equations (2.1-2.3) along with the above boundary conditions(2.4-2.6) are solved for the fluid flow and heat transfer over a Rotating heated circular cylinder obstacle to obtain velocity, pressure and temperature fields.

Once the velocity and temperature fields are obtained, the Local Nusselt number is defined as

$$Nu = \frac{hH}{k} = -\frac{\partial c}{\partial n} \tag{2.7}$$

where $h$ represents the local heat transfer coefficient and k denotes the thermal conductivity of air.

## 3. Finite element method and Implementation

To construct a time discretization scheme for the Navier-Stokes equations (2.1-2.3) with boundary conditions (2.4-2.6). Our choice is a Fully-implicit Crank-Nicolson scheme as described in [19] for retaining the basic non-linearity in the Navier-Stokes equations. The time-centered Crank-Nicolson scheme gives nonlinear equations to be solved at each time

level and redefining $\mathbf{u}$ to be the velocity at the new time level and $\mathbf{u_1}$ the velocity at the previous time level, we arrive at these spatial problems:

$$\begin{aligned} \operatorname{div}\mathbf{U} &= 0 \\ \frac{\mathbf{u}-\mathbf{u_1}}{\Delta t} + \mathbf{u_1}\cdot\nabla\mathbf{u_1} &= -\nabla p + \frac{1}{Re}\Delta\mathbf{U} \\ \frac{c-c_1}{\Delta t} + \mathbf{U}\cdot\nabla C &= \frac{1}{RePr}\Delta C \end{aligned}$$

with

$$\mathbf{U} = \frac{1}{2}(\mathbf{u}+\mathbf{u_1}), \quad C = \frac{1}{2}(c+c_1)$$

denoting the arithmetic averages needed in a Crank-Nicolson time integration. The corresponding variational formulation involves the integrals

$$\begin{aligned} \int_\Omega ((\frac{\mathbf{u}-\mathbf{u_1}}{\Delta t})v_u + (\mathbf{u_1}\cdot\nabla\mathbf{u_1}).v_u - p\nabla\cdot v_u \\ + \frac{1}{Re}\nabla\mathbf{U}:\nabla v_u + v_p\nabla\cdot\mathbf{U})dx = 0 \\ \int_\Omega ((\frac{c-c_1}{\Delta t})v_c + (\mathbf{U}\cdot\nabla C).v_c \\ + \frac{1}{RePr}(\nabla C.\nabla v_c))dx = 0 \end{aligned} \tag{3.1}$$

where $v_u, v_p$ and $v_c$ are test functions for the test spaces of $u, p$, and $c$ respectively.

Finite element software basically has to solve three sub-problems namely, Mesh generation, system-matrix assembly and solution of the resulting linear systems of equations. We use Mshr for mesh generation and FEniCS [18] for matrix assembly and the solution of linear systems. A Continuous Galerkin (CG) finite elements are used to discretize the velocity and pressure components by quadratic and linear polynomials respectively, and CG-quadratic finite elements are used for temperature. A completely different strategy would be used to solve for velocity, pressure and temperature simultaneously by coupled solver using MixedFunctionSpace. CBC.PDESys is built upon the finite element package FEniCS [18](Logg et al., 2012). FEniCS is a powerful development environment for performing finite element modeling, including strong support for symbolic automatic differentiation, native parallel support and parallel interface with linear algebra solvers such as PETSc (Balay et al.,) and Trillinos (Heroux et al.,) and automatic code generation and compilation for compiled performance from an interpreted language interface. The Python scripting environment makes the generation and linking of new code straightforward. A finite element method consisting of 17157 vertices and 32816 triangles as shown in figure 2, is used in this study. The numerical code is first checked against the benchmarked results for the backward facing step.

### 3.1 Validation study

The numerical solution procedure used here has been benchmarked with standard results for backward facing step reported in the literature [14–17]. The Table 1 shows the validation of reattachment length devided by the step hight for Reynolds number Re=100 and ER=2. The minimum deviation for the percentage in the error is obtained for the results of [15] is found to be about 0.3 percent, whereas the maximum deviation is around 2.74 percent. This validates the present numerical solution, the comparison results shows good overall agreement and slight differences for higher Reynolds number. This difference is believed to be due to the differences in the domain and grid sizes used by others as opposed to the present study.

**Figure 2**

| **Author** | $X_R/S$ |
|---|---|
| Present study | 4.98 |
| Lin et al.[14] | 4.91 |
| Acharya et al.[15] | 4.97 |
| Cochran et al.[16] | 5.32 |
| Dyne et al.[17] | 4.89 |

**Table 1** Validation of the present solver with existing study at Re=100 and ER=2

## 4. Results and Discussion

The main parameters that effect the fluid flow and thermal characteristics are Reynolds number, Prandtl number, step height, distance between the step edge to the channel exit, distance between the inlet to the step edge, cylinder position and diameter, expansion ratio and cylinder rotation angle. In the current study, the numerical simulations are performed for the Reynolds number ($1 \leq Re \leq 200$), cylinder rotation angle($-3 \leq \omega \leq 3$) and vertical locations ($b = 0.5S, S, 1.5S$) of the obstacle from the bottom wall of the channel are examined for fluid flow and heat transfer enhancement over a backward facing step flow.

### 4.1 Effects of cylinder rotation angle

Figs.3 and 4 indicates that the effect of varying cylinder rotation angle($\omega$) on the streamlines and isotherms at blockage ratio of 20 percentage for fixed values of Reynolds number 100 and Prandtl number 0.71. In the absence of the cylinder obstacle as time is increased, the flow at the edge of the step separates and a recirculation zone is observed behind the step (Figs. 3a, 3b). The size of this zone increases with an increase in time. Further more no recirculation zoze is occur in the channel till the Reynold number Re=5. The case $\omega = 0$ corresponds to a stationary cylinder which is shown in Figs. 3c and 3d. In this case, streamlines are slightly deflected towards the the gap between the bottom wall and bottom part of the cylinder spacing in the presence of the motionless cylinder

and several vortices appear behind the step and in the vicinity of the cylinder close to the bottom wall. A recirculation zone is also seen on the bottom wall of the channel see Fig. 3d.

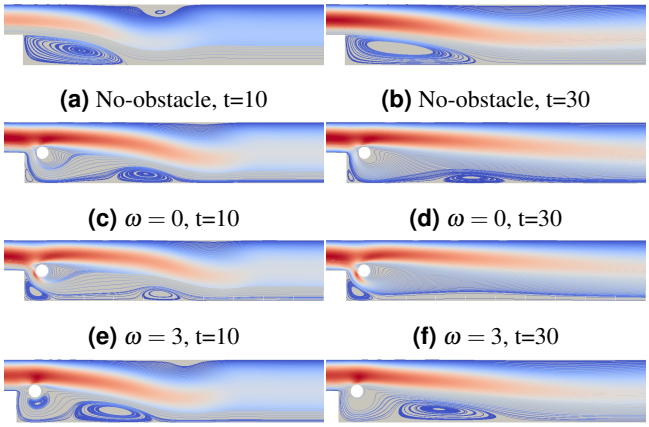

**(a)** No-obstacle, t=10 **(b)** No-obstacle, t=30

**(c)** $\omega = 0$, t=10 **(d)** $\omega = 0$, t=30

**(e)** $\omega = 3$, t=10 **(f)** $\omega = 3$, t=30

**(g)** $\omega = -3$, t=10 **(h)** $\omega = -3$, t=30

**Figure 3.** Effect of cylinder rotation angle on the streamlines for fixed value of Re=100, b=H

A positive value of the rotation ($\omega$) indicates counter clockwise rotation of the cylinder Figs.3e and 3f. When the cylinder rotates in this direction, more flow is accelerated towards between the step and cylinder due to the combined effect of contraction area and rotation. The motion of the fluid flowing through the top of the cylinder and the size of the recirculation zone on the bottom channel wall are affected compared to motionless cylinder case. The flow structure near the bottom and right of the cylinder are affected to some extent.

When the cylinder rotates in the clockwise direction (negative value of $\omega$ )Figs. 3g and 3h, flow is accelerated in the region between the upper channel wall and the cylinder due to the contraction effect. Some portion of the flow is directed towards the bottom of the cylinder and related to this effect, the vortex appear on the bottom of the cylinder for motionless cylinder case disappears. The size and extent of the recirculation bubble appearing behind the step decreases compared to motionless cylinder case Fig. 3h. The flow separation is delayed with cylinder rotation angle $\omega$.

Figs. 4 shows the isotherms profiles for the without obstacle, motionless and rotating cylindrical obstacle case for Reynolds number Re=100. When the cylinder rotates in clockwise direction, less clustering of the isotherms for the top surface due to the recirculation region and indicates poor heat transfer characteristic for this region since more flow is directed towards the spacing between the upper channel wall and cylinder. For counter clockwise rotation direction, the isotherms fluctuates more on the upper wall and right and bottom parts of the cylinder due to the formation of the vortices compared to motionless cylinder case.

The effect of varying cylinder rotation angles on the local Nusselt number distributions along the surfaces of the bottom wall is demonstrated in Fig.5 for Re = 100 at position

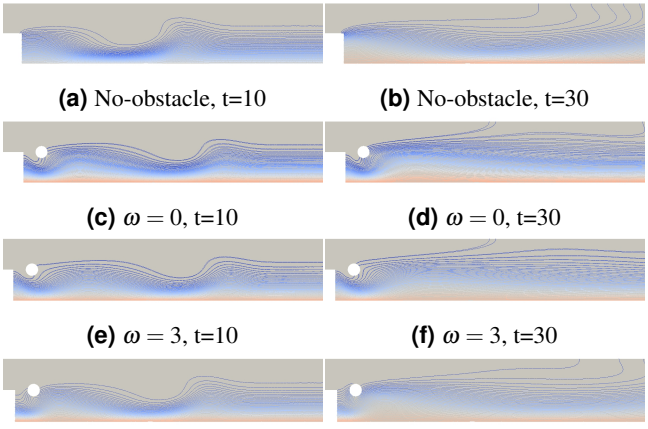

**(a)** No-obstacle, t=10 **(b)** No-obstacle, t=30

**(c)** $\omega = 0$, t=10 **(d)** $\omega = 0$, t=30

**(e)** $\omega = 3$, t=10 **(f)** $\omega = 3$, t=30

**(g)** $\omega = -3$, t=10 **(h)** $\omega = -3$, t=30

**Figure 4.** Effect of cylinder rotation angle on the isotherms for fixed value of Re=100, b=H

b=1S. Introducing an cylinder obstacle (motionless or rotating) enhances the thermal transport form the rear surface of the backstep geometry due to the flow acceleration towards the gap between the step and the cylinder obstacle.

For counter clockwise rotation of cylinder $\omega = 3$, the location of the maximum heat transfer changes as can be seen in Fig. 5. Since more flow is entrained into the recirculation zone of the rotating circular cylinder and deflection of the flow patterns upwards on the top of the obstacle for the counter clockwise rotation of the cylinder, heat transfer is less effective on this surface. The peaks in the Nusselt number corresponds to reattachment points of recirculation zones. For clockwise rotation of the cylinder, the peaks in the Nusselt number increase compared to motionless cylinder case due to the entrainment of the fluid flow in the cylinder wake and in the gap between the bottom wall and bottom part of the cylinder. For higher Reynolds numbers, there is slightly change of peak value of the Nusselt number and its location with cylinder rotation compared to motionless cylinder case.

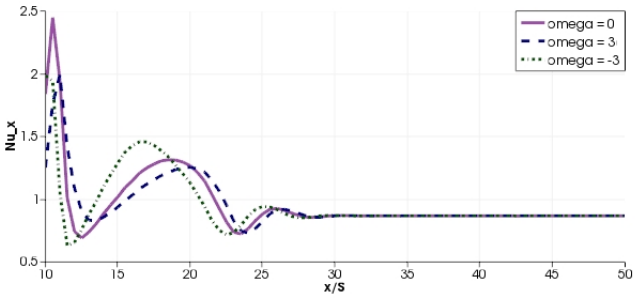


**Figure 5.** Variation of Local Nusselt number with different values of cylinder rotation angle at Reynolds number = 100

## 4.2 Effects of Reynolds number

Figs. 6 and 7 indicates the effect of varying Reynolds numbers on the flow and thermal patterns at fixed values of $\omega = 3$ and different time level. At Reynolds number of 100, some

portion of the fluid separated from the bottom wall again separates behind the cylinder obstacle as seen in Figs. 6c and 6d. As Reynolds number increases, the flow separated form the bottom wall is entrained into the wake of the cylinder obstacle and formation of the vortices is seen behind the cylinder obstacle shown in Figs. 6c, 6d, 6e and 6f. Further, it is observed that at the highest value of Reynolds number of 200, there is the formation of a secondary separation bubble on the bottom wall of the step geometry Figs. 6e and 6f.

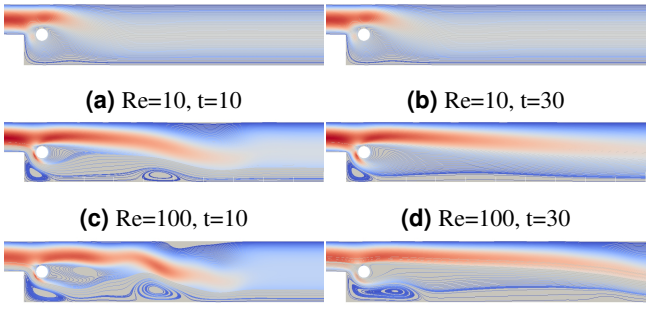

**(a)** Re=10, t=10 **(b)** Re=10, t=30

**(c)** Re=100, t=10 **(d)** Re=100, t=30

**(e)** Re=200, t=10 **(f)** Re=200, t=30

**Figure 6.** Effect of Reynolds number on the streamlines for $\omega = 3$

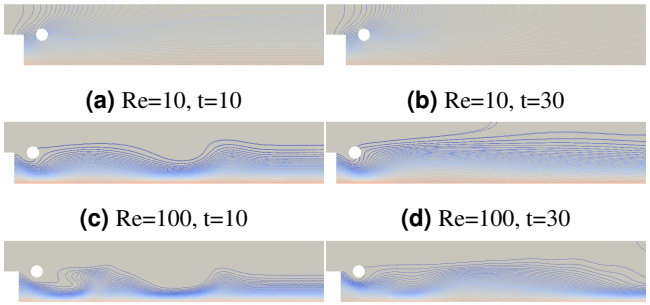

**(a)** Re=10, t=10 **(b)** Re=10, t=30

**(c)** Re=100, t=10 **(d)** Re=100, t=30

**(e)** Re=200, t=10 **(f)** Re=200, t=30

**Figure 7.** Effect of Reynolds number on the isotherms for $\omega = 3$

The effect of varying Reynolds number on the local Nusselt number for cylinder rotation angle $\omega = 3$ is demonstrated in Fig. 8 at position b=1. From this figure it can be generalized that the maximum Nusselt values increase with an increase in the Reynolds number. At Re = 100 and 200, the second peak corresponds to reattachment of the recirculation bubble on the bottom wall of the channel. The effect of cylinder rotation angle on the local Nusselt number distribution is more pronounced at low Reynolds number. At Re = 10, the maximum and average heat transfer increase with cylinder rotation.

### 4.3 Effects of cylinder positions

Figs. 9 and 10 demonstrate the effect of empty channel, channel with cylinder obstacle position and rotation angle on the streamlines and isotherms for fixed value of Reynold number

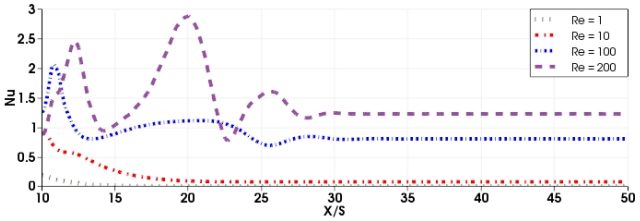


**Figure 8.** Effect of Reynolds number on the local Nusselt number for cylinder rotation angle $\omega = 3$

100. For the case without the installation of the cylinder obstacle, as time is gradually increased, the flow separates at the edge of the step and a closed primary recirculation region is observed behind the step for a fixed value of the expansion ratio. Further downstream of the reattachment points, the flow regains its fully developed flow behavior.

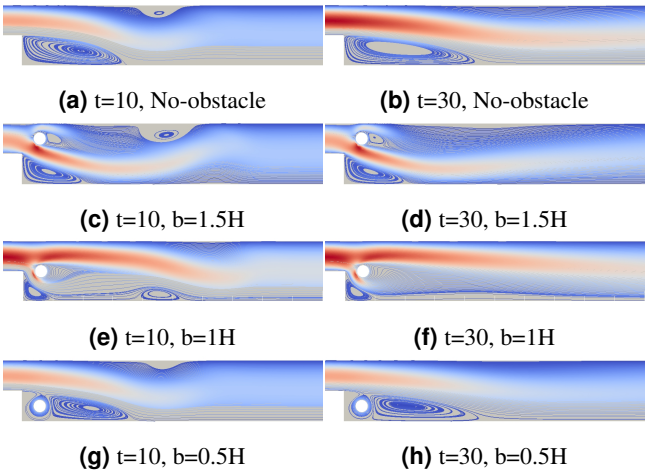

**(a)** t=10, No-obstacle **(b)** t=30, No-obstacle

**(c)** t=10, b=1.5H **(d)** t=30, b=1.5H

**(e)** t=10, b=1H **(f)** t=30, b=1H

**(g)** t=10, b=0.5H **(h)** t=30, b=0.5H

**Figure 9.** Effect of cylinder position on the streamlines for fixed value Re=100, $\omega = 3$

When the obstacle is mounted behind the step for the location at b = 0.5S, the effect on the flow patterns on the upstream side is negligible for all Reynolds number since the flow coming from the upstream of the step is not considerably affected by the cylinder obstacle. Therefore, the separation on streamlines from the top corner of the step resemble in behavior the counterparts for the unobstructed case as can be seen in Figs. 9g and 9h. For the obstacle location at b = 1.0S, more flow is directed towards the step and bottom wall downstream of the step, the reattachment occurs at the location upstream of the reattachment locations compared to the case obstacle at b=0.5S and the motion of fluid flowing over the cylinder is found to be affected to some extent. Related to this effect as can be clearly observed from Figs. 6f and 9f, the reattachment of discrete vortices in the primary recirculation zone adjacent to the step occurs at a position clearly upstream of the corresponding positions observed in the cases of unobstructed flow and the flow at b= 0.5S. As can be seen in Fig. 9f, the stream line representing this fluid motion moves down and once reattaches the bottom surface. But it separates from the

bottom surface and is entrained into the wake of the cylinder. Therefore, a secondary separation bubble appears downstream of the primary reattachment point.

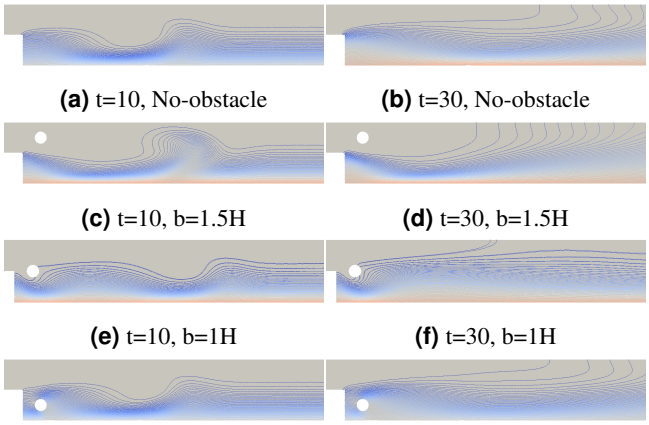

**(a)** t=10, No-obstacle **(b)** t=30, No-obstacle

**(c)** t=10, b=1.5H **(d)** t=30, b=1.5H

**(e)** t=10, b=1H **(f)** t=30, b=1H

**(g)** t=10, b=0.5H **(h)** t=30, b=0.5H

**Figure 10.** Effect of cylinder position on the isotherms for fixed value Re=100, $\omega = 3$

When the cylinder at b=1.5S, a huge amount of fluid moves through the gap between the top corner of the step and the cylinder obstacle. In this case, some portion of the fluid separated from the bottom wall again separates behind the cylinder obstacle and the length of the recirculation zone behind the step increases compared to the case b=H and b=0.5S. For the case b=0.5S, 1.5S and no-obstacle, the appearance of a secondary recirculation region on the upper wall can also be observed (Figs. 9a, 9c,9g) at t=10 for Reynolds number Re=100 and rotation angle $\omega = 3$. This case also presents a significant compression of the stream lines deflected beneath the circular cylinder and two circulating cells are formed behind the cylinder object as shown in Fig. 9d.

As it can be seen in Figs. 10a and 10b), under the influence of the reattaching flow, the temperature contours for the case of unobstructed flow undergo local compression around the flow-reattachment point. The thermal boundary layer is compressed by the reattaching wall-ward flow. As a result, a layer with steep temperature gradient is formed above the wall around the flow reattachment point, which leads to heat transfer enhancement there.

As it can be seen from Fig.10, cylinder obstacle alters the temperature contours. Comparing with unobstructed flow, isotherms for the case of b=0.5S (Figs. 10g and 10h) is found that there is not any significant variation except for the slight distortion of the isotherms in the vicinity of the circular cylinder. This is complemented by the similarity in flow patterns for the two cases. In this case, isotherm patterns are directed from the step towards the left of the cylinder obstacle for Reynolds number of 100. When the obstacle is located at b = 1.0S as shown in Figs. 10e and 10f the location where the steep temperature gradient occurs moves upstream when compared to the case b=0.5S. However, there is only one point of compression corresponding to the reattachment point of the primary recirculation zone and lies significantly upstream compared to its other counterparts.

For the cylinder obstacle position at b = 1.5S (Figs. 10c and 10d), the temperature contours depict a marked compression and crowding of the isotherms below the cylinder and close to the reattachment point of the primary recirculation zone. The isotherms further get compressed at another point downstream that lies close to the reattachment point of the secondary separation bubble. The effects are more pronounced at higher values of the flow Reynolds number. For this position more clustering of the isotherms is seen on the bottom wall downstream of the step. Further, there is excessive congestion of isotherm lines on that side of the cylinder that directly obstructs the flow compared to its rear side.

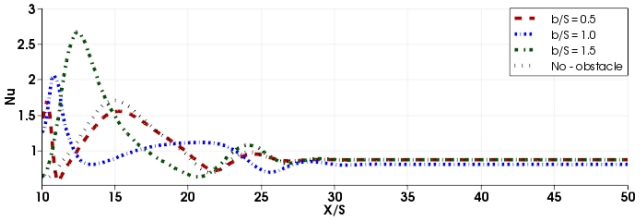


**(a)**

**Figure 11.** Effect of cylinder position on the local Nusselt number for cylinder rotation angle $\omega = 3$ at Reynolds number = 100

Fig. 11 shows that the local Nusselt number along the bottom wall for the four different position of the flow configurations considered for cylinder rotation angle $\omega = 3$ at Reynolds number = 100. This figure shows that the local number Nusselt variation for the unobstructed flow, and as can be seen from the graph that there exists a peak in the Nusselt number that corresponds to a point close to the flow reattachment point. For the case b = 0.5S does not show any significant variation in the nature of the local number Nusselt plots compared to the unobstructed flow. However there is a slight distortion in the initial parts of the plot owing to the presence of the circular cylinder in the flow separation zone. For the case b = 1.0S and b = 1.5S illustrate a drastic enhancement in the peak Nusselt values as compared to the other cases. This is attributed to the enhanced compression of the thermal boundary layer by the adiabatic circular cylinder in the backward-facing step geometry. The first higher peak corresponding to the reattachment point of the primary recirculation zone and the second lower peak corresponding to the reattachment of the secondary separation bubble. The case b = 1.5S shows only one peak in the Nusselt number value on account of the lone recirculation zone in this geometry. For higher Reynolds numbers, there is slightly change of peak value of the Nusselt number and its location with cylinder rotation compared to motionless cylinder case.

### 4.4 Conclusion

A laminar flow over a backward facing step channel in the presence of a rotating circular cylinder placed behind the step is numerically studied. The effect of cylinder rotation angle $(-3 \leq \omega \leq 3)$, Reynolds number $(1 \leq Re \leq 200)$ and obstacle location (b = 0.5S, S, 1.5S) on the fluid flow and heat transfer characteristics are numerically investigated.

The present numerical methodology has been extensively validated against previous numerical and experimental studies found in the literature. The grid and computational domain were chosen after extensive testing by varying various grid and domain sizes. Detailed observations of flow pattern, recirculation length, local Nusselt number for the onset of flow separation along the bottom wall have been presented.

Length and intensity of the recirculation zone behind the step are considerably affected with the installation of the cylinder obstacle positions and it can be controlled with rotation angle. As Reynolds number increases, local Nusselt number also increase on particular angle of rotation. When the cylinder rotates in the clockwise direction, more flow is entrained into the wake of the cylinder and some portion of the flow is directed towards the bottom of the cylinder and related to this effects the size and extent of the recirculation bubble appearing on the upper wall and on the bottom of the cylinder are affected. Adding the cylinder obstacle alters the isotherm plots. It is seen that there is significant change on the clustering of the isotherm patterns and the location where this steep temperature gradient occurs in the flow with the installation of the cylinder obstacle. It has been demonstrated that the insertion of a circular cylinder is effective for altering the velocity field of the backward-facing flow if the cylinder is positioned at the appropriate position. This change in the flow characteristics results in a heat transfer enhancement across the bottom surface of the step. Further, it is also found that the peak and average values of the Nusselt number increase monotonically with increase in the Reynolds number.

## References


[1] B.F. Armaly, A. Li, J.H. Nie, *Measurements in three-dimensional laminar separated flow*, Int. J. Heat Mass Transfer 46 (19) (2003) 3573-3582.

[2] H. Stuer, A. Gyr, W. Kinzelbach, *Laminar separation on a forward facing step*, European Journal of Mechanics—B/Fluids 18 (1999) 675-692.

[3] B.F. Armaly, F. Durst, J.C.F. Pereier, B. Schonung, *Experimental and theoretical investigation of backward-facing step flow*, Journal of Fluid Mechanics 127 (1983) 473-496.

[4] M. Sherry , D.LoJacono, and J.Sheridan, *An experimental investigation of the recirculation zone formed downstream of a forward facing step*, J. Wind Eng.Ind.Aerodyn., 98(2010) 888-894.

[5] A. Anguraj and J. Palraj, *Comparison of four different obstacle models of fluid flow with a slip-like boundary condition*. Malaya J. Mat. 2(4)(2014) 517-526.

[6] H. Abu-Mulaweh, *A review of research on laminar mixed convection flow over backward- and forward facing steps*, Int. J. Therm. Sci. 42 (2003) 897-909.

[7] J. Nie, B. Armaly, *Three-dimensional convective flow adjacent to backwardfacing step-effects of step height*, Int. J. Heat Mass Transfer 45 (2002) 2431-2438.

[8] Barbosa-Saldana JG, Anand NK. *Flow over a three-dimensional horizontal forward-facing step*. Numer Heat Transfer A 53 (2008) 1-17.

[9] F. Rehimi, F. Aloui, S. Ben Nasrallah, L. Doubliez, J. Legrand, *Experimental investigation of a confined flow downstream of a circular cylinder centred between two parallel walls,* J. Fluids Struct. 24 (2008) 855-882.

[10] S.H. Hussain, A.K. Hussein, *Mixed convection heat transfer in a differentially heated square enclosure with a conductive rotating circular cylinder at different vertical locations,* Int. Commun. Heat Mass Transf. 38 (2011) 263-274.

[11] Selimefendigil F, Oztop H. *Control of laminar pulsating flow and heat transfer in backward facing step by using a square obstacle*. ASME-J Heat Transf 136 (2014)081701.

[12] H.F. Oztop, K.S. Mushatetb, I. Yilmaz, *Analysis of turbulent flow and heat transfer over a double forward facing step with obstacles*, International Communications in Heat and Mass Transfer 39 (2012) 1395-1403.

[13] A. Kumar, A.K. Dhiman, *Effect of a circular cylinder on separated forced convection at a backward-facing step,* Int. J. Therm. Sci. 52 (2012) 176-185.

[14] J.T. Lin, B.F. Armaly, T.S. Chen, *Mixed convection in buoyancy-assisting vertical backward-facing step flows*, Int. J. Heat Mass Transfer 10 (1990) 2121-2132.

[15] S. Acharya, G. Dixit, Q. Hou, *Laminar mixed convection in a vertical channel with a backstep: a benchmark study*, ASME HTD 258 (1993) 11-20.

[16] R. Cochran, R. Horstman, Y. Sun, A. Emery, *Benchmark solution for a vertical buoyancy-assisted laminar backward-facing step flow using finite element, finite volume and finite difference methods*, ASME HTD 258 (1993) 37-47.

[17] B. Dyne, D. Pepper, F. Brueckner, *Mixed convection in a vertical channel with a backward-facing step*, ASME HTD 258 (1993).

[18] A. Logg, K.A. Mardal, G.N. Wells, et al., *Automated Solution of Differential Equations by the Finite Element Method*, Springer, 2012.

[19] R. Eymard, T. Gallouet and R. Herbin, *Finite Volume Methods, Handbook of Numerical Analysis*, 7 (2003) 713-1020. Edited by P.G. Ciarlet and J.L. Lions (North Holland).



★★★★★★★★★

ISSN(P):2319 – 3786

Malaya Journal of Matematik

ISSN(O):2321 – 5666

★★★★★★★★★